

Precise SMEFT predictions for di-Higgs production

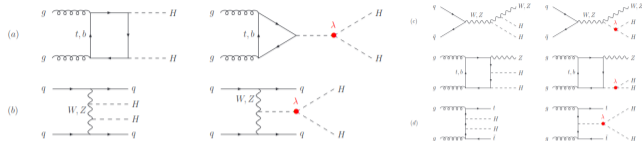
Higgs Physics: Part 2, Thursday ~4:12 pm

Jannis Lang mainly based on [\[2204.13045\]](#) with Gudrun Heinrich and Ludovic Scyboz | May 25, 2023

INSTITUTE FOR THEORETICAL PHYSICS



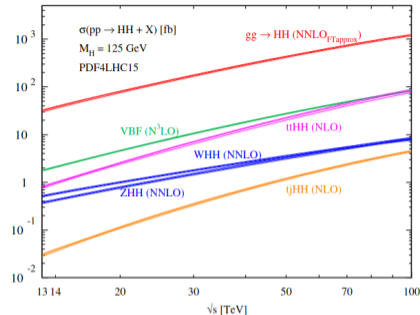
What do we mean by “precise SMEFT predictions”?



[1910.00012]

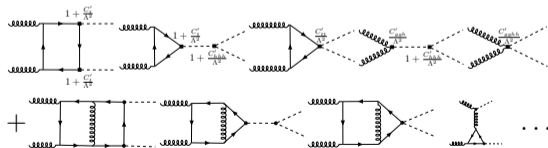
- Selection of hh channels

→ Only consider $gg \rightarrow hh$ channel



- Higher order corrections by SM couplings (explicit loops)

→ NLO QCD corrections



What do we mean by “precise SMEFT predictions”?

- Higher order terms in (defining) EFT expansion parameter

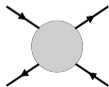
$$\mathcal{L}_{SMEFT} = \mathcal{L}_{SM} + \sum_i \frac{C_i^{(6)}}{\Lambda^2} \mathcal{O}_i^{(6)} + \mathcal{O}(\Lambda^{-4})$$

→ Only dim-6 operators considered (leading order in Λ^{-2})

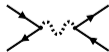
- Assigning additional hierarchy to EFT Wilson coefficients (UV assumption)

$$U_l(3) \times U_e(3) \times U_Q(2) \times U_t(2) \times U_d(3)$$

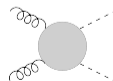
→ Stringent Flavor assumption ($m_f := 0$, except m_t), differentiating potentially tree- with strictly loop-induced operators (implicit loop factor in Wilson coefficient)



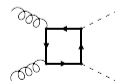
←



VS.



←



Two bottom-up EFT systematics: SMEFT vs. HEFT

- SMEFT:**
- Linear Higgs sector: light Higgs contained in EW doublet field $\phi(x)$
 - Canonical counting, truncate expansion at Λ^{-2} (only CP even operators)

$$\begin{aligned}
 \mathcal{L}_{\text{SMEFT}}^{(\text{Warsaw})} \supset & \frac{C_{H\Box}}{\Lambda^2} (\phi^\dagger \phi) \Box (\phi^\dagger \phi) + \frac{C_{HD}}{\Lambda^2} (\phi^\dagger D_\mu \phi) (\phi^\dagger D^\mu \phi) + \frac{C_H}{\Lambda^2} (\phi^\dagger \phi)^3 \\
 & + \frac{C_{uH}}{\Lambda^2} \left((\phi^\dagger \phi) \bar{q}_L \tilde{\phi} t_R + \text{h.c.} \right) + \frac{C_{HG}}{\Lambda^2} (\phi^\dagger \phi) G_{\mu\nu}^a G^{a\mu\nu} + \underbrace{\frac{C_{uG}}{\Lambda^2} \left(\bar{q}_L \sigma^{\mu\nu} T^a G_{\mu\nu}^a \tilde{\phi} t_R + \text{h.c.} \right)}_{\text{subdominant (UV assumption)} \rightarrow \text{last part}}
 \end{aligned}$$

- HEFT:**
- Non-linear theory (EW χ L), motivation as analogue to chiral pert. theory
 - Light Higgs is EW gauge singlet
 - Expansion in $\frac{f^2}{\Lambda^2} \sim \frac{1}{16\pi^2}$ (\Rightarrow loop counting)

$$\mathcal{L}_{\text{HEFT}} \supset \underbrace{-m_t \left(c_t \frac{h}{v} + c_{tt} \frac{h^2}{v^2} \right) \bar{t}t - c_{hhh} \frac{m_h^2}{2v} h^3}_{\subset \mathcal{L}_{\text{HEFT}}^{\text{LO}}} + \underbrace{\frac{\alpha_s}{8\pi} \left(c_{ggh} \frac{h}{v} + c_{gggh} \frac{h^2}{v^2} \right) G_{\mu\nu}^a G^{a\mu\nu}}_{\subset \mathcal{L}_{\text{HEFT}}^{\text{NLO}}}$$

\Rightarrow Classically non-renormalisable, but consistent if truncations are considered at each step!

Two bottom-up EFT systematics: SMEFT vs. HEFT

SMEFT:

$$\mathcal{L}_{SMEFT}^{(Warsaw)} \supset \frac{C_{H\Box}}{\Lambda^2} (\phi^\dagger \phi) \Box (\phi^\dagger \phi) + \frac{C_{HD}}{\Lambda^2} (\phi^\dagger D_\mu \phi) (\phi^\dagger D^\mu \phi) + \frac{C_H}{\Lambda^2} (\phi^\dagger \phi)^3$$

$$+ \frac{C_{uH}}{\Lambda^2} \left((\phi^\dagger \phi) \bar{q}_L \tilde{\phi} t_R + \text{h.c.} \right) + \frac{C_{HG}}{\Lambda^2} (\phi^\dagger \phi) G_{\mu\nu}^a G^{a\mu\nu}$$

HEFT:

$$\mathcal{L}_{HEFT} \supset -m_t \left(c_t \frac{h}{v} + c_{tt} \frac{h^2}{v^2} \right) \bar{t}t - c_{hhh} \frac{m_h^2}{2v} h^3 + \frac{\alpha_s}{8\pi} \left(c_{ggh} \frac{h}{v} + c_{gghh} \frac{h^2}{v^2} \right) G_{\mu\nu}^a G^{a\mu\nu}$$

Naive translation SMEFT \leftrightarrow HEFT after field redefinition up to $\mathcal{O}(\Lambda^{-2})$ in Lagrangian
 ($C_{H,kin} = C_{H\Box} - 4C_{HD}$)

However, formally:

$$c_i \sim \mathcal{O}(1) \text{ possible} \quad \leftrightarrow \quad \frac{E^2}{\Lambda^2} C_i \ll 1$$

\Rightarrow Not generally applicable in practical calculations
 (fits, bounds, ...)

HEFT	Warsaw
C_{hhh}	$1 - 2 \frac{v^2}{\Lambda^2} \frac{v^2}{m_h^2} C_H + 3 \frac{v^2}{\Lambda^2} C_{H,kin}$
C_t	$1 + \frac{v^2}{\Lambda^2} C_{H,kin} - \frac{v^2}{\Lambda^2} \frac{v}{\sqrt{2}m_t} C_{uH}$
C_{tt}	$-\frac{v^2}{\Lambda^2} \frac{3v}{2\sqrt{2}m_t} C_{uH} + \frac{v^2}{\Lambda^2} C_{H,kin}$
C_{ggh}	$\frac{v^2}{\Lambda^2} \frac{8\pi}{\alpha_s(\mu)} C_{HG}$
C_{gghh}	$\frac{v^2}{\Lambda^2} \frac{4\pi}{\alpha_s(\mu)} C_{HG}$

SMEFT truncation

Dimension 6 operators in amplitude ($\frac{C'_i}{\Lambda^2} = C_i - C_{i,sm}$):

$$\begin{aligned}
 \mathcal{M} = & \text{[SM diagram]} + \text{[SI diagram]} + \text{[diagonal diagram]} + \text{[dim6^2 diagram 1]} + \text{[dim6^2 diagram 2]} + \dots \\
 = & \mathcal{M}_{\text{SM}} + \underbrace{\frac{1}{\Lambda^2} \mathcal{M}_{\text{si}}}_{\text{dim6}} \left(+ \underbrace{\frac{1}{\Lambda^4} \mathcal{M}_{\text{di}}}_{\text{dim6}^2} \right)
 \end{aligned}$$

- ⇒ Double operator insertion same order as (neglected) dimension 8 operators (and field redefinition)!
- ⇒ In HEFT the complete anomalous coupling enters at each vertex with no additional truncation

SMEFT truncation of cross section

$$\sigma \simeq \left\{ \begin{array}{l} \sigma_{\text{SM}} + \sigma_{\text{SM} \times \text{dim6}} \\ \sigma_{(\text{SM} + \text{dim6}) \times (\text{SM} + \text{dim6})} \\ \sigma_{(\text{SM} + \text{dim6}) \times (\text{SM} + \text{dim6})} + \sigma_{\text{SM} \times \text{dim6}^2} \\ \sigma_{(\text{SM} + \text{dim6} + \text{dim6}^2) \times (\text{SM} + \text{dim6} + \text{dim6}^2)} \end{array} \right.$$

(a) Truncation at leading order of expansion of powers in Λ^{-2} of cross section \Rightarrow applicable choice

(b) Truncation at leading order of expansion of powers in Λ^{-2} of amplitude \Rightarrow applicable choice

(c) Truncate cross section at $\mathcal{O}(\Lambda^{-4})$ from all dim6 operator insertions (ambiguous definition)

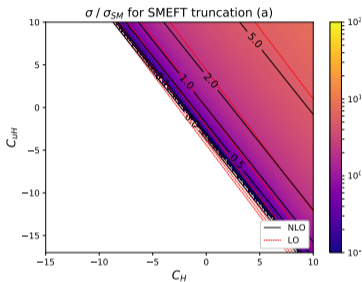
(d) Complete insertion, naive translation SMEFT \leftrightarrow HEFT

- Truncation (a) formally most consistent, however, negative (differential) cross section can appear for too large Wilson coefficients

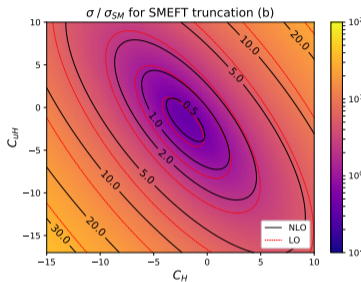
\Rightarrow Perform analysis for truncation (a) and (b) separately!

NLO cross section heatmaps in SMEFT

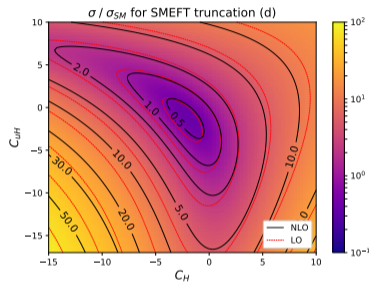
Generated at $\sqrt{s} = 13$ TeV with $\Lambda = 1$ TeV



(a)



(b)



(d)

- Large area of negative cross section for truncation (a)
- Flat directions differ substantially
- Non-trivial shape for HEFT-like option (d)

Public implementations

HEFT

HTL = Heavy top limit ($m_t \rightarrow \infty$)

- LO and NLO QCD HTL HPAIR [Gröber,Mühlleitner,Spira,Streicher '15]

- Full m_t NLO QCD POWHEG-BOX-V2/ggHH
 - [Borowka,Greiner,Heinrich,Jones,Kerner,Schlenk,Zirke '16]
 - [Heinrich,Jones,Kerner,Luisoni,Vryonidou '17]
 - [Buchalla,Capozzi,Celis,Heinrich,Scyboz '18]
 - [Heinrich,Jones,Kerner,Luisoni,Scyboz '19]
 - [Heinrich,Jones,Kerner,Scyboz '20] ←

- **Non-public** state-of-the-art NNLO' (HTL NNLO, full m_t NLO) [de Florian,Fabre,Heinrich,Mazitelli,Scyboz '21]

SMEFT

- LO and NLO QCD HTL HPAIR [Gröber,Mühlleitner,Spira,Streicher '15]

- LO (1-loop) including chromo-magnetic operator
 SMEFT@NLO + MG5_aMC@NLO [Degrande,Durieux,Maltoni,Mimasu,Vryonidou,Zhang '20]

- LO including chromo-magnetic operator
 SMEFTsim + MG5_aMC@NLO [Brivio,Jiang,Trott '17]
[Brivio '20]

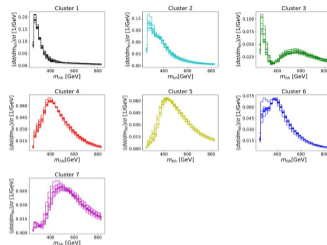
- Full m_t NLO QCD POWHEG-BOX-V2/ggHH_SMEFT
 with truncation options [Heinrich,JL,Scyboz '22] ←

Naive benchmark translation

Consider HEFT benchmark points with following characteristic m_{hh} shapes

[Capozi, Heinrich '19]
[<https://cds.cern.ch/record/2843280>]

- Benchmark 1*: enhanced low m_{hh} region
- Benchmark 6*: close-by double peaks or shoulder left



benchmark (* = modified)	C_{hhh}	C_t	C_{tt}	C_{ggh}	C_{gggh}	$C_{H,kin}$	C_H	C_{uH}	C_{HG}	Λ
SM	1	1	0	0	0	0	0	0	0	1 TeV
1*	5.105	1.1	0	0	0	4.95	-6.81	3.28	0	1 TeV
6*	-0.684	0.9	$-\frac{1}{6}$	0.5	0.25	0.561	3.80	2.20	0.0387	1 TeV

⇒ SMEFT expansion based on $E^2 \frac{C_i}{\Lambda^2} \ll 1$ justified?

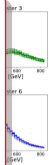
C_{HG} obtained using $\alpha_s(m_Z) = 0.118$

Naive benchmark translation

Total cross section generated at $\sqrt{s} = 13$ TeV

Con
with

benchmark	$\sigma_{\text{NLO}}[\text{fb}]$ option (b)	K-factor option (b)	ratio to SM option (b)	$\sigma_{\text{NLO}}[\text{fb}]$ option (a)	$\sigma_{\text{NLO}}[\text{fb}]$ HEFT
SM	$27.94^{+13.7\%}_{-12.8\%}$	1.67	1	-	-
$\Lambda = 1$ TeV					
1*	$74.29^{+19.8\%}_{-15.6\%}$	2.13	2.66	-61.17	94.32
6*	$72.51^{+20.6\%}_{-16.4\%}$	1.90	2.60	52.89	91.40
$\Lambda = 2$ TeV					
1*	$14.03^{+12.0\%}_{-11.9\%}$	1.56	0.502	5.58	-
6*	$35.39^{+17.5\%}_{-15.2\%}$	1.76	1.27	34.18	-



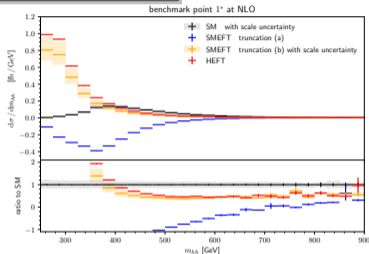
⇒ SMEFT expansion based on $E^2 \frac{C_i}{\Lambda^2} \ll 1$ justified?

Invariant mass distributions at NLO QCD ($\sqrt{s} = 13 \text{ TeV}$)

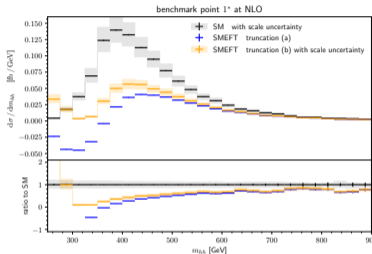
Benchmark 1*:

C_{hh}	C_t	C_{tt}	C_{ggh}	C_{gggh}	$C_{H,\text{kin}}$	C_H	C_{uH}	C_{HG}
5.105	1.1	0	0	0	4.95	-6.81	3.28	0

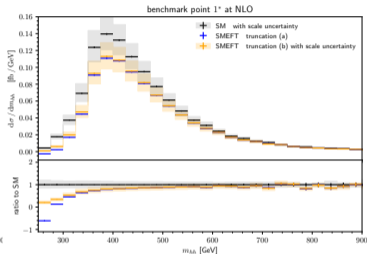
Generated with ggHH_SMEFT in POWHEG-BOX-V2



$\Lambda = 1 \text{ TeV}$



$\Lambda = 2 \text{ TeV}$



$\Lambda = 4 \text{ TeV}$

■ Truncation (a): negative cross sections

■ Shape approaches SM for increasing Λ

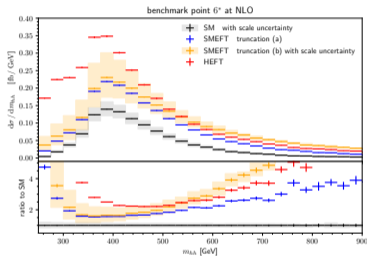
⇒ Valid HEFT point invalid in SMEFT after direct translation

Invariant mass distributions at NLO QCD ($\sqrt{s} = 13 \text{ TeV}$)

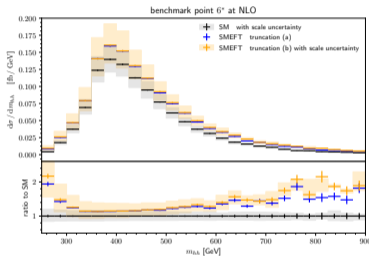
Benchmark 6*:

Generated with ggHH_SMEFT
in POWHEG-BOX-V2

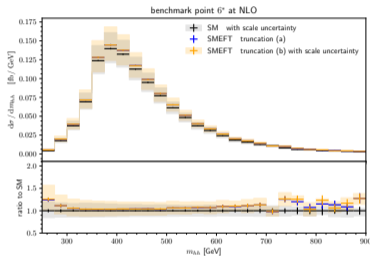
C_{hhh}	C_t	C_{tt}	C_{ggh}	C_{gggh}	$C_{H,kin}$	C_H	C_{uH}	C_{HG}
-0.684	0.9	$-\frac{1}{6}$	0.5	0.25	0.561	3.80	2.20	0.0387



$\Lambda = 1 \text{ TeV}$



$\Lambda = 2 \text{ TeV}$



$\Lambda = 4 \text{ TeV}$

- No negative cross section
- No shoulder left

- Shape indistinguishable from SM for $\Lambda = 4 \text{ TeV}$ within scale uncertainties

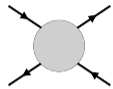
$$\Delta\sigma \sim \begin{matrix} +\Delta_{\text{scale}} + \\ -\Delta_{\text{scale}} - \end{matrix} \begin{matrix} +\Delta_{m_t \text{ scheme}} + \\ -\Delta_{m_t \text{ scheme}} - \end{matrix} \pm \Delta_{\text{num. grid}} \quad (\pm \Delta_{\text{EFT trunc.}}) \quad \pm \Delta_{\text{PDF}+\alpha_s} \quad \pm \Delta_{\text{EW}}$$

- Δ_{EW} : Full NLO EW unknown, only partial results of top Yukawa [Davies, Mishima, Schönwald, Steinhauser, Zhang '22] [Mühlleitner, Schlenk, Spira '22]
- $\Delta_{\text{PDF}+\alpha_s} \approx 3\%$ ($\sqrt{s} = 13 \text{ TeV}$): B.I. NNLO HTL and employing PDF4LHCNNLO [twiki *hh* cross group] stable for c_{hhh} variation, but might rise if tail enhanced
- $\Delta_{\text{EFT trunc.}}$: No quantitative prescription, qualitative observation of truncation options
- $\Delta_{\text{scale}} \pm$: Determined by 7-point variation of $\mu_R, \mu_F = \{0.5, 1, 2\} \cdot \mu_0$
 $\mathcal{O}(15\%)$ for NLO QCD SM, 15 - 20% for NLO QCD SMEFT truncation (b) benchmark 1* & 6*
- $\Delta_{m_t \text{ scheme}} \pm$: In principle needs determination for each point in EFT parameter space! (not yet available) [Baglio et al '18] [Baglio et al '20] [Baglio et al '20]
- $\Delta_{\text{num. grid}}$: Numerical uncertainty of grids for virtual contribution, not covered by Monte Carlo statistical uncertainty of POWHEG!

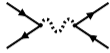
Loop counting in SMEFT (“weak” UV assumption)

Assuming UV is renormalisable QFT leads to: [Arzt, Einhorn, Wudka '94] [Buchalla, Heinrich, Müller-Salditt, Pandler '22]

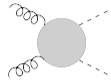
(κ generic weak coupling, $d_\chi(\partial, \bar{\psi}\psi, \kappa) = 1$)



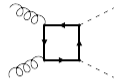
←



VS.



←



$$\mathcal{O}_{tH} \sim [\kappa^3] (\phi^\dagger \phi) \bar{q}_L \tilde{\phi} t_R$$

$$\Rightarrow \frac{C_{tH}}{\Lambda^2} \sim \frac{1}{\Lambda^2}$$

$$\mathcal{O}_{HG} \sim [\kappa^4] (\phi^\dagger \phi) G_{\mu\nu}^a G^{a\mu\nu}$$

$$\Rightarrow \frac{C_{HG}}{\Lambda^2} \sim \frac{1}{\Lambda^2 (16\pi^2)}$$

$$\mathcal{O}_{tt} \sim [\kappa^2] \bar{t}_R \gamma_\mu t_R \bar{t}_R \gamma^\mu t_R$$

$$\Rightarrow \frac{C_{tt}}{\Lambda^2} \sim \frac{1}{\Lambda^2}$$

$$\mathcal{O}_{tG} \sim [\kappa^4] (\bar{q}_L \sigma^{\mu\nu} T^a t_R) \tilde{\phi} G_{\mu\nu}^a$$

$$\Rightarrow \frac{C_{tG}}{\Lambda^2} \sim \frac{1}{\Lambda^2 (16\pi^2)}$$

⇒ Chromomagnetic operator enters at same order as 2-loop 4-fermion operator contribution:

$$\left[\begin{array}{c} \text{Diagram 1: 2-loop 4-fermion operator} \\ \text{Diagram 2: 2-loop 4-fermion operator with Higgs} \end{array} \right]_{\text{si}} \sim \frac{1}{\Lambda^2 (16\pi^2)}$$

$$\left[\begin{array}{c} \text{Diagram 3: 2-loop 4-fermion operator with Higgs} \\ \text{Diagram 4: 2-loop 4-fermion operator with Higgs} \end{array} \right] \sim \frac{1}{\Lambda^2 (16\pi^2)^2}$$

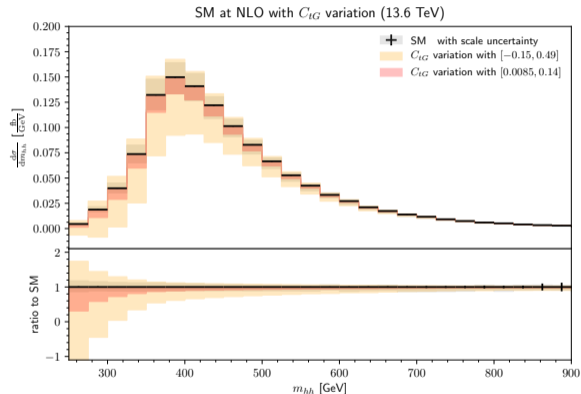
Work in progress!

Effects of chromomagnetic operator (PRELIMINARY)

- SM with C_{tG} variation using $\mathcal{O}(\Lambda^{-2})$ constraints from [SMEFiT Collaboration, Ethier et al '21]:

C_{tG}	
individual	marginalised
$g_s [0.007, 0.111]$	$g_s [-0.127, 0.403]$

- Better constrained by other processes

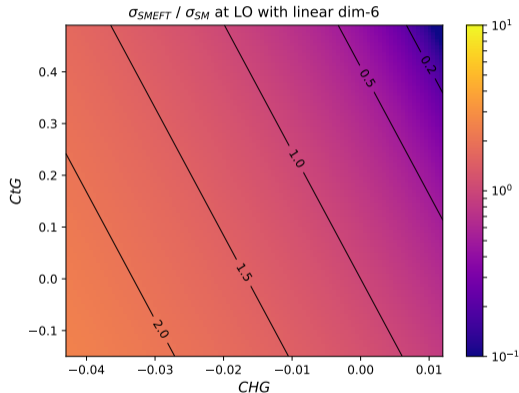


Effects of chromomagnetic operator (PRELIMINARY)

- SM with C_{tG} variation using $\mathcal{O}(\Lambda^{-2})$ constraints from [SMEFiT Collaboration, Ethier et al '21]:

C_{tG}	
individual	marginalised
$g_s [0.007, 0.111]$	$g_s [-0.127, 0.403]$

- Better constrained by other processes

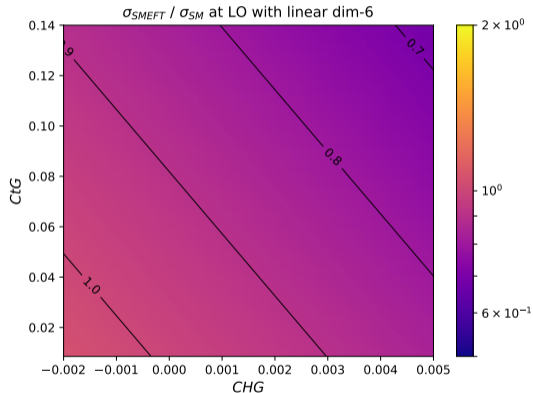


Effects of chromomagnetic operator (PRELIMINARY)

- SM with C_{tG} variation using $\mathcal{O}(\Lambda^{-2})$ constraints from [SMEFiT Collaboration, Ethier et al '21]:

C_{tG}	
individual	marginalised
$g_s [0.007, 0.111]$	$g_s [-0.127, 0.403]$

- Better constrained by other processes



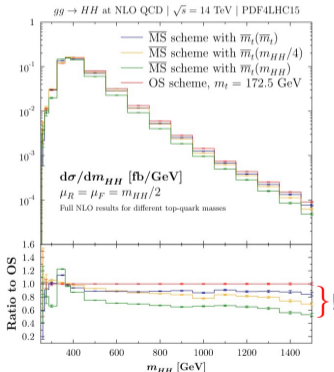
- Status of SMEFT precision in di-Higgs (ggF)
 - SMEFT and HEFT both valid EFT approaches based on different assumptions
 - BM study: Naive translation from HEFT \rightarrow SMEFT can lead out of validity of $\frac{1}{\Lambda^2}$ expansion
- \Rightarrow We advocate to study both EFT representations separately
- More information about this project: [\[Heinrich,JL,Scyboz '22\]](#)
 - More information about EFT in Higgs pair production: [\[https://cds.cern.ch/record/2843280\]](https://cds.cern.ch/record/2843280)
- \Rightarrow In progress: Inclusion of chromo-magnetic and 4-fermion operator contributions, RGE evolution of Wilson coefficients (expected to be relevant, see e.g. [\[2212.05067\]](#) [\[2109.02987\]](#) . . .)
- \Rightarrow Further outlook: y_b effects and EW corrections when SM results are available, . . .

m_t renormalisation scheme uncertainty

[Baglio,Campanario,Glaus,Mühlleitner,Spira,Streicher '18]
 [Baglio,Campanario,Glaus,Mühlleitner,Ronca,Spira,Streicher '20]
 [Baglio,Campanario,Glaus,Mühlleitner,Ronca,Spira '20]

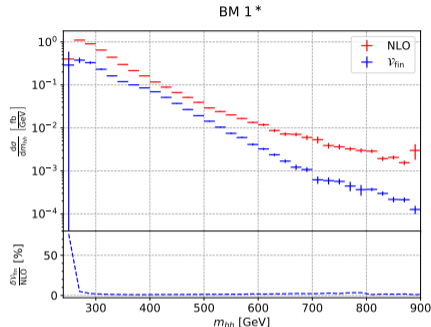
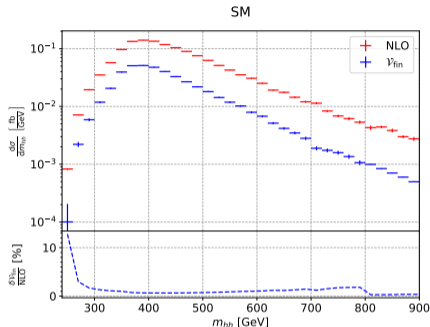
$$\bar{m}_t(m_t) = \frac{m_t}{1 + \frac{4}{3} \frac{\alpha_s(m_t)}{\pi} + K_2 \left(\frac{\alpha_s(m_t)}{\pi} \right)^2 + K_3 \left(\frac{\alpha_s(m_t)}{\pi} \right)^3}$$

- Prediction depends on m_t scheme (on-shell vs. \overline{MS} with varying scale)
- Uncertainty sensitive to choice of $C_{hhh} = \kappa_\lambda$
- Sensitivity to variations of C_{tt} expected



$\kappa_\lambda = -10$:	$\sigma_{tot} = 1438(1)_{-6\%}^{+10\%}$ fb,
$\kappa_\lambda = -5$:	$\sigma_{tot} = 512.8(3)_{-7\%}^{+10\%}$ fb,
$\kappa_\lambda = -1$:	$\sigma_{tot} = 113.66(7)_{-9\%}^{+8\%}$ fb,
$\kappa_\lambda = 0$:	$\sigma_{tot} = 61.22(6)_{-12\%}^{+6\%}$ fb,
$\kappa_\lambda = 1$:	$\sigma_{tot} = 27.73(7)_{-18\%}^{+4\%}$ fb,
$\kappa_\lambda = 2$:	$\sigma_{tot} = 13.2(1)_{-23\%}^{+1\%}$ fb,
$\kappa_\lambda = 2.4$:	$\sigma_{tot} = 12.7(1)_{-22\%}^{+4\%}$ fb,
$\kappa_\lambda = 3$:	$\sigma_{tot} = 17.6(1)_{-15\%}^{+9\%}$ fb,
$\kappa_\lambda = 5$:	$\sigma_{tot} = 83.2(3)_{-4\%}^{+13\%}$ fb,
$\kappa_\lambda = 10$:	$\sigma_{tot} = 579(1)_{-4\%}^{+12\%}$ fb

Numerical grids uncertainty

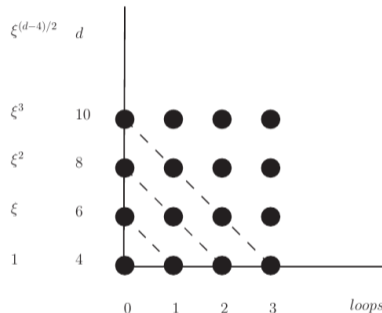


- Low (and high) m_{hh} region very sparsely populated in virtual grids, due to small contribution in SM
- ⇒ $\mathcal{O}(12\%)$ uncertainty for SM in first bin not represented by Monte Carlo statistical uncertainty in POWHEG
- ⇒ Uncertainty much worse for scenarios with enhanced low m_{hh} region

EFT systematics: canonical vs. loop counting

$$\xi = \frac{v^2}{f^2}$$
$$\frac{f^2}{\Lambda^2} \sim \frac{1}{16\pi^2}$$

- Canonical counting in rows, valid if $\xi \ll \frac{f^2}{\Lambda^2}$
- Loop counting in columns, valid if $\xi \sim 1$



[Buchalla,Catà,Krause 14']

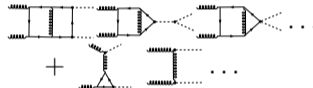
Amplitude evaluation in ggHH_SMEFT

$$\mathcal{M}_{gg \rightarrow hh} = \epsilon(p_1)_\mu \epsilon(p_2)_\nu (\mathcal{F}_1 \cdot T_1^{\mu\nu} + \mathcal{F}_2 \cdot T_2^{\mu\nu}) \quad [\text{Glover, van der Bij '87}]$$

Born: Analytic expressions for form factors \mathcal{F}_1 and \mathcal{F}_2 (tree and 1-loop contributions)

Real: $|\mathcal{M}_{gg \rightarrow hhg}|^2$, $|\mathcal{M}_{qg \rightarrow hhq}|^2$, $|\mathcal{M}_{q\bar{q} \rightarrow hhg}|^2$ and crossings evaluated using (private) modified version of **GoSam** 1-loop ME generator

Virtual: 2-loop diagrams in HEFT are similar to SM \Rightarrow reweighting



HEFT virtuals are available as function of 23 grids a_j

$$\begin{aligned} |\mathcal{M}_{gg \rightarrow hh}^{NLO}|^2 = & a_1 \cdot c_t^4 + a_2 \cdot c_{tt}^2 + a_3 \cdot c_t^2 c_{hhh}^2 + a_4 \cdot c_{ggh}^2 c_{hhh}^2 + a_5 \cdot c_{ggh}^2 + a_6 \cdot c_{tt} c_t^2 + a_7 \cdot c_t^3 c_{hhh} \\ & + a_8 \cdot c_{tt} c_t c_{hhh} + a_9 \cdot c_{tt} c_{ggh} c_{hhh} + a_{10} \cdot c_{tt} c_{ggh} + a_{11} \cdot c_t^2 c_{ggh} c_{hhh} + a_{12} \cdot c_t^2 c_{ggh} \\ & + a_{13} \cdot c_t c_{hhh}^2 c_{ggh} + a_{14} \cdot c_t c_{hhh} c_{ggh} + a_{15} \cdot c_{ggh} c_{hhh} c_{ggh} + a_{16} \cdot c_t^3 c_{ggh} \\ & + a_{17} \cdot c_t c_{tt} c_{ggh} + a_{18} \cdot c_t c_{ggh}^2 c_{hhh} + a_{19} \cdot c_t c_{ggh} c_{ggh} + a_{20} \cdot c_t^2 c_{ggh} \\ & + a_{21} \cdot c_{tt} c_{ggh}^2 + a_{22} \cdot c_{ggh}^3 c_{hhh} + a_{23} \cdot c_{ggh}^2 c_{ggh} \end{aligned}$$

\Rightarrow Grids can be directly reused for SMEFT (considering translation and truncation) up to counter terms and special treatment for truncation (b), where additional 1-loop contributions are added

Virtual grids for ggHH_SMEFT

Split matrix in kinematic part times coupling coefficient for HEFT and SMEFT

$$\begin{aligned}\mathcal{M}_{LO} &:= m_1 \cdot c_t^2 + m_2 \cdot c_t c_{hhh} + m_3 \cdot c_{tt} + m_4 \cdot c_g c_{hhh} + m_5 \cdot c_{gg} \\ &= m_1 + m_2 + \frac{1}{\Lambda^2} \left(2m_1 \cdot C_t' + m_2 \cdot (C_t' + C_{hhh}') + m_3 \cdot C_{tt}' + m_4 \cdot C_g' + m_5 \cdot C_{gg}' \right) + \frac{1}{\Lambda^4} \left(m_1 \cdot C_t'^2 + m_2 \cdot C_t' C_{hhh}' \right) \\ \mathcal{M}_{NLO} &:= M_1 \cdot c_t^2 + M_2 \cdot c_t c_{hhh} + M_3 \cdot c_{tt} + M_4 \cdot c_g c_{hhh} + M_5 \cdot c_{gg} + M_6 \cdot c_g^2 + M_7 \cdot c_g c_t \\ &= M_1 + M_2 + \frac{1}{\Lambda^2} \left(2M_1 \cdot C_t' + M_2 \cdot (C_t' + C_{hhh}') + M_3 \cdot C_{tt}' + M_4 \cdot C_g' + M_5 \cdot C_{gg}' + M_7 \cdot C_g' \right) \\ &\quad + \frac{1}{\Lambda^4} \left(M_1 \cdot C_t'^2 + M_2 \cdot C_t' C_{hhh}' + M_6 \cdot C_g'^2 + M_7 \cdot C_g' C_t' \right)\end{aligned}$$

The virtual grids, given as kinematic coefficients a_i of the squared matrix element

$$\begin{aligned}|\mathcal{M}_{NLO}|^2 &= a_1 \cdot c_t^4 + a_2 \cdot c_{tt}^2 + a_3 \cdot c_t^2 c_{hhh}^2 + a_4 \cdot c_{ggh}^2 c_{hhh}^2 + a_5 \cdot c_{ggh}^2 + a_6 \cdot c_{tt} c_t^2 + a_7 \cdot c_t^3 c_{hhh} + a_8 \cdot c_{tt} c_t c_{hhh} + a_9 \cdot c_{tt} c_{ggh} c_{hhh} \\ &\quad + a_{10} \cdot c_{tt} c_{gghh} + a_{11} \cdot c_t^2 c_{ggh} c_{hhh} + a_{12} \cdot c_t^2 c_{gghh} + a_{13} \cdot c_t c_{hhh}^2 c_{ggh} + a_{14} \cdot c_t c_{hhh} c_{gghh} + a_{15} \cdot c_{ggh} c_{hhh} c_{gghh} + a_{16} \cdot c_t^3 c_{ggh} \\ &\quad + a_{17} \cdot c_t c_{tt} c_{ggh} + a_{18} \cdot c_t c_{ggh}^2 c_{hhh} + a_{19} \cdot c_t c_{ggh} c_{gghh} + a_{20} \cdot c_t^2 c_{ggh}^2 + a_{21} \cdot c_{tt} c_{ggh}^2 + a_{22} \cdot c_{ggh}^3 c_{hhh} + a_{23} \cdot c_{ggh}^2 c_{gghh},\end{aligned}$$

can be understood as combinations of $m_i \times M_j$ obtained from $\mathcal{M}_{LO} \times \mathcal{M}_{NLO}$. After rearrangement, the squared matrix elements entering the truncated cross sections in SMEFT (slide 7) are expressed in terms of the same a_i , except for truncation (b), where

$$\Delta\sigma_{(b)} = m_2 \times M_4 \cdot \frac{C_{ggh}'(C_{hhh}' - C_t')}{\Lambda^4} + m_4 \times M_7 \frac{C_{ggh}'^2}{\Lambda^4}$$

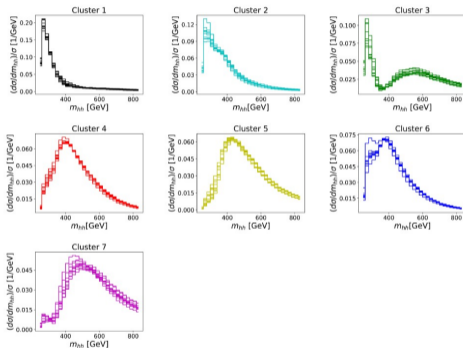
needs to be added.

Updated HEFT benchmarks

[<https://cds.cern.ch/record/2843280>]

benchmark	C_{hhh}	C_t	C_{tt}	C_{ggh}	C_{gggh}
SM	1	1	0	0	0
1*	5.105	1.1	0	0	0
2*	6.842	1.033	$\frac{1}{6}$	$-\frac{1}{3}$	0
3	2.21	1.05	$-\frac{1}{3}$	0.5	0.5
4*	2.79	0.9	$-\frac{1}{6}$	$-\frac{1}{3}$	$-\frac{1}{2}$
5	3.95	1.17	$-\frac{1}{3}$	$\frac{1}{6}$	$-\frac{1}{2}$
6*	-0.684	0.9	$-\frac{1}{6}$	0.5	0.25
7	-0.10	0.94	1	$\frac{1}{6}$	$-\frac{1}{6}$

- Shape clusters defined using unsupervised ML
- Benchmarks chosen with clear shape features and satisfying experimental constraints
- * denotes updated benchmark point, new constraints:
 $0.83 \leq c_t \leq 1.17$ (and $|c_{tt}| \leq 0.05$ for 1*)



[Capozi, Heinrich '19]